ZigBee-Based Communication System for Data Transfer Within Future Microgrids

Made A. Setiawan, *Student Member, IEEE*, Farhad Shahnia, *Member, IEEE*, Sumedha Rajakaruna, *Member, IEEE,* and Arindam Ghosh, *Fellow, IEEE*

***Abstract*—A wireless data communication system for future microgrids (MGs) is presented in this paper. It is assumed that each MG has a central controller and each distributed generation unit in the MG has a local controller. The communication system is responsible for transmitting and receiving data amongst these controllers. This communication system is based on ZigBee technology, which is a low cost and low power consumption device. However, its main limitation is the low data transfer rate. To reduce the number of data transactions, a data management scheme is presented in this paper. The required data to be transferred are defined and a suitable coding is proposed. Finally, the number of transmitted symbols and the processing time of the proposed data management scheme are numerically analyzed. In addition, the dynamic operation of an MG is evaluated considering the delays that are imposed by this communication system.**

***Index Terms*—Communication system, data management scheme, data transmission delay, microgrids (MGs), ZigBee.**

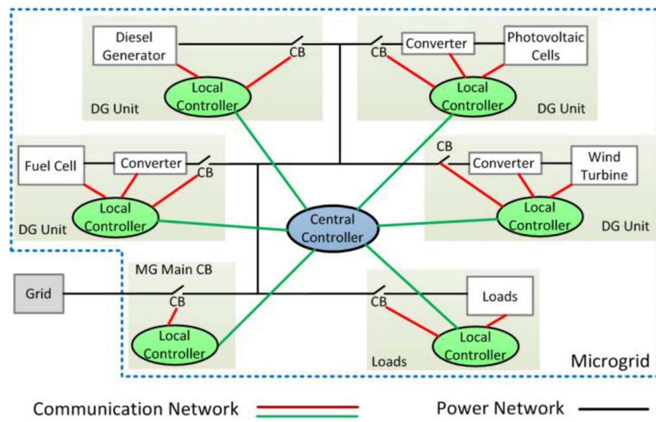

Fig. 1. Schematic of a MG system.

I. Introduction

THE INCREASING number of renewable energy resources such as photovoltaic, wind, and micro-hydro are leading to a substantial amount of electric energy generation in the form of distributed generation (DG) units within the electric networks. Integration of the DGs will benefit the electric networks by reducing the network expansion costs, minimizing the power losses in long feeders and increasing the reliability of the network. It may also be helpful to achieve faster recovery following a fault in the network [1].

Microgrid (MG) is a cluster of loads, DGs and energy storages interconnected by a network of feeders and located in the same geographical area. It can act as an independent power system whenever needed. In the presence of a utility grid, an MG can operate either in grid-connected mode or in autonomous mode. In grid-connected mode, the network voltage and frequency are dictated by the grid; hence the DGs are controlled such that the desired amount of power (based on maximum power point tracking or economic power dispatch) is supplied by each DG. Hence, any power mismatch between the power generated by the DGs and the load requirement will be met by the grid. In autonomous mode, the DGs are not only required to supply the MG load demand but should also regulate the feeder voltage and frequency within acceptable limits. Therefore, for proper operation and control of DGs within an MG, each DG should be updated with the information about the MG operating mode. This information is required to be transferred from the MG main circuit breaker (CB) that connects the MG and the grid (see Fig. 1), to all the DGs.

Additionally, the MG requires the real-time power measurement of the grid, loads and DGs as well as the state of charge (SoC) of the available energy storage devices. Similarly, the root mean square (RMS) value, phase angle, and frequency of voltage as well as the active/reactive power at certain specific points in the MG are required to be monitored and given as inputs to the DG control systems. Furthermore, instantaneous values of voltages at the terminals of DGs and the feeder are needed for synchronizing a new DG with the MG. Fig. 1 shows a sample MG network along with the different data which need to be monitored and transmitted to the respective controllers.

It is expected that in the near future all the operations in an MG will be fully automated [2]. A comparison of the characteristics of the present and future MG systems is presented in Table I. The automation system of the future MGs includes fetching data from the sensors, passing the data to the controllers and finally passing the control commands to the

Manuscript received August 14, 2014; revised January 2, 2015; accepted February 4, 2015. Date of publication February 27, 2015; date of current version August 19, 2015. This work was supported by Lembaga Pengelola Dana Pendidikan, Ministry of Finance, Indonesia. Paper no. TSG-00814-2014.

M. A. Setiawan is with the Politeknik Manufaktur Negeri Bangka Belitung, Sungailiat 33211, Indonesia.

F. Shahnia, S. Rajakaruna, and A. Ghosh are with the Department of Electrical and Computer Engineering, Curtin University, Perth, WA 6102, Australia (e-mail: farhad.shahnia@curtin.edu.au).

Color versions of one or more of the figures in this paper are available online at http://ieeexplore.ieee.org.

Digital Object Identifier 10.1109/TSG.2015.2402678

TABLE I
CHARACTERISTICS OF THE PRESENT AND FUTURE MGS

Present	Future
Decentralized control	Centralized/Distributed control
Little monitoring	Self/automated monitoring
Few sensors	A lot of sensors and actuators
Limited information for customer	Full information for customers
Electromechanical equipment	Digital equipment
Unidirectional communication	Bidirectional communication
Data accessed centrally	Data accessed in multiple centers
Manual restoration	Semi/full automated restoration
Manual prediction	Real-time data prediction
Fixed-setting protection systems	Adaptive protection systems

actuators. Therefore, MGs need a fast and accurate data transmission system to transfer the measured data and command signals to the relevant controllers [3].

Wired and wireless communication technologies can be employed in MGs. The popular wired technologies, used in power systems, are serial communication RS-232/422/485, bus technology (e.g., ModBus, ProfiBus, and CANBus) [4], power-line communication (e.g., distribution line carrier, power line communication, and broadband power line communication) [3], and Ethernet (e.g., LAN and optical cable) [4], [5]. On the other hand, the popular wireless technologies, used in power systems, are cellular (e.g., global system for mobile communications and code division multiple access) [5], Wi-Fi [6], [7], WiMax [8], ZigBee [9]–[11], Z-Wave [12], Bluetooth [10], Insteon [13], radio frequency [10], and Microwave [13].

The wired technologies have a higher data transfer bandwidth and are more reliable; however, their installation cost is relatively high. On the other hand, the wireless technologies have lower installation costs and are more suitable for remote areas. At the same time, they are more flexible for future expansions [10]. A comparison among different wireless technologies that can be considered for MG applications is presented in Table II.

Due to the growing number of meters, sensors, and actuators which needs to be monitored and controlled continuously within an MG, utilizing wired technologies leads to a significant installation cost. Therefore, the wireless technologies are a better candidate for MG applications. However, it is to be noted that they have a lower data transmission rate and may also be vulnerable to interferences with other signals [7].

In this paper, a ZigBee-based communication technology is proposed for data transfer in MGs. ZigBee has been widely considered for data transmission in power systems. In [14], ZigBee is used for data monitoring of all subsystems of a dc MG system. It is also used for real-time measurement and data transfer in a power system application in [15], where an algorithm is proposed for compressing the data.

The reliability of ZigBee technology in power system applications, including the number of good and bad data packets transmitted under impulsive high power transients, are evaluated in [16]. In addition, an encryption code is developed for ZigBee in [9] to increase the security of the transmitted data.

Since the data transfer rate for ZigBee is low, to reduce the need for high data transfer by such a device, a data traffic scheduling scheme is proposed in [17] where the data traffics are prioritized into three classifications, each with smaller packet sizes. Alternatively, the need for high data bandwidth can be reduced by using a distributed algorithm in a ZigBee cluster-tree network [18] or a multiinterface management framework [19] or by coordinating data traffic diffusion [20].

Implementation of ZigBee as a wireless sensor network is proposed in [21], in which a WiFi-ZigBee message delivery scheme is developed to reduce the power consumption of the wireless devices. Also, an algorithm is developed in [22] to avoid interference between ZigBee and WiFi signals, when both are used in power system applications.

In [23], a simple data coding is presented for ZigBee which consists of one byte of data format, two bytes of data length, and variable bytes of data itself. The limitation of this method is that it is suitable for transferring only one data. The ZigBee data payload coding has not been yet addressed for different data transfers that are required in MGs.

In [24], ZigBee processing time is calculated to be about 400–600 μs for transmitting three different data; however, there is no statement of the utilized data coding format. In MG applications, the delay of data transmission is crucial and must be kept within an acceptable limit. Additionally, this delay depends on the utilized data coding and the length of data code. Since longer data codes have longer transmission delays, defining a suitable and efficient data coding method, which represents all data transactions for MG operations, is crucial.

In this paper, a suitable data payload code and a data management scheme is proposed for a ZigBee-based communication technology for MGs. In addition, the effect of the communication delay is evaluated on the dynamic performance of the MG. The main contributions of this paper are as follows:

1) proposing a ZigBee-based data communication technology for MG applications;
2) developing an organized data management scheme;
3) developing a suitable data payload code;
4) numerically analyzing the total data processing delay and number of transmitted symbols and evaluating MG dynamic performance in the presence of communication delays.

The rest of this paper is organized as follows. Section II discusses the different communication layers required in MGs. ZigBee-based communication technology for MGs is proposed in Section III. A data management scheme for MGs is presented in Section IV, while the data processing delay is discussed in Section V. Some numerical results are presented in Section VI to demonstrate the number of transmitted symbols and the required transmission delay in MGs. Section VII demonstrates the communication delay effects on the dynamic performance of an MG. The general conclusion of this paper is summarized in the last section.

II. COMMUNICATION LAYERS IN MGS

A hierarchical control system is required for the proper operation and control of the MG, as discussed below.

1) *The Local (Primary) Controller:* This controller is the lowest control block within the hierarchical control

TABLE II
TECHNICAL COMPARISON OF DIFFERENT WIRELESS TECHNOLOGIES APPLICABLE FOR MGs

Technology	Range	Rate	Frequency	Routing	Security	Suitable for	Modulation	Initial Costs
Cellular	several km	270 kbps	900, 1800 MHz (2G), 2.1 GHz (3G)	Direct	64 bit A5/1, KASUMI cipher (3G)	backbone	GMSK	Costly
WiFi	100 m	54 Mbps	2.4 GHz	more than 70 protocols	WPA	backbone	QPSK, BPSK, 16/64 QAM.	moderate
WiMax	several km	30-40 Mbps	2.3, 2.5, 3.5 GHz	AODV, DSR, OLSR, ZRP	AES and 3DES	backbone	BPSK, QPSK, 16/64QAM, OFDMA-PHY	moderate
ZigBee	100-1500 m	250 kbps	2,4 GHz, 868, 915 MHz	AODV, HERA	AES	end devices	OQPSK, BPSK	low
Z-Wave	30 m	100 kbps	900 MHz	source-routed mesh network	Unique ID	end devices	GFSK	low
Insteon	50 m	38 kbps	900 MHz	Send and receive	Unique ID	end devices, backbone	BPSK	low
Bluetooth	100 m	24 Mbps	2.4 GHz	a master-slave structure	encryption key	end devices, backbone	GFSK, DQPSK and 8DPSK	low

system and is located within every DG unit. This controller mainly controls the operation of a DG based on its local measurements. Hence, it fetches data from the local sensors/meters using very small sampling time steps and produces the required outputs for the DG actuators. During grid-connected mode of operation of the MG, the DG units operate in constant PQ mode and generate their rated power or operate based on maximum power point technique. In autonomous mode, the DGs need to operate in droop control. This is briefly introduced in the Appendix and discussed in details in [25].

2) *The MG Central Controller:* This is the main controller for the MG and is responsible for controlling the voltage magnitude and frequency in the MG. This controller receives the voltage magnitude, angle, and frequency data from the voltage sensor installed at the MG feeder and sends back the proper references of the voltage magnitude and angle to each DG. This controller has a larger time step compared to the local controllers and operates discontinuously (in steps of a few minutes). In addition, the transfer of the MG main CB status to the MG central controller falls within this control level.
3) *The Network Tertiary Controller:* This controller is the highest control level in the hierarchical control system and is responsible for general control of the power network. This controller may have several modules such as load/weather forecast, electricity market, self-healing, unit-commitment, economic dispatch, etc. This controller also defines if an MG should be operating in grid-connected or autonomous mode, the output power of each DG unit, the interconnection/isolation of two neighboring MGs, etc.

To provide a proper data transmission among the abovementioned three controllers, a communication network and infrastructure are required.

The main data to be transferred from the local controllers of each DG to the MG central controller are the voltage magnitude/angle and output active/reactive power and the DG CB status. In addition to these, the MG main CB status and the voltage magnitude and frequency within the MG (measured at one or more locations) need to be transferred to the MG central controller.

To transfer these data to the MG central controller, several parameters should be considered in selecting and designing the communication technology. They are as follows:

1) the size of the area in which the MG is distributed;
2) the installation, operational, and maintenance costs;
3) the number of sensors, actuators, meters, or devices;
4) the minimum data transmission rate requirement;
5) the data precision requirement;
6) the maximum data packet error requirement;
7) the flexibility to future expansions;
8) the availability of different techniques to access data.

Based on the location of the communication devices as well as the characteristics of the data to be transferred, the communication technologies in the MG are classified in three layers, as shown schematically in Fig. 2. The first communication layer provides data transfer capability among the local controller of each DG to the sensors, meters, and actuators of the DG unit. In addition, the transfer of data from any meters/sensors installed along the power distribution lines or CBs to their local controllers also falls within this layer. The second communication layer provides data transfer capability among the local controllers of the DGs and the MG central controller. This layer is the main communication layer of the MG. The third communication layer is used to provide data transfer within a group of neighboring MGs [25]–[27] This layer transfers data between the central controllers of the MGs and the electric network tertiary controller. This paper focuses on the MG second communication layer only.

It is to be noted that a decentralized control of an MG is also possible. However, the hierarchical control system discussed in this paper broadens the network operating capabilities. On the other hand, implementation of the hierarchical control system and the required communication infrastructure increases the complexity of the system control and the investment costs. Therefore, a techno-economic analysis can be carried out to define the balance between the imposed costs and complexity and the gained benefits. This is beyond the scope of this research and is not considered in this paper.

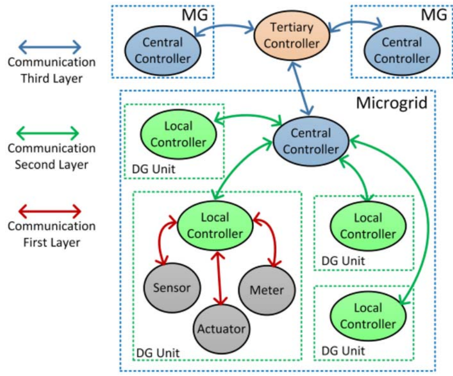

Fig. 2. Proposed hierarchical communication layer in MG.

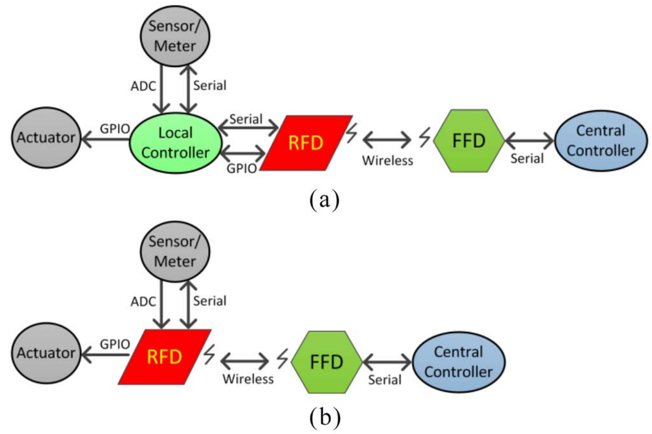

Fig. 3. FFD and RFD utilization in the MG. (a) DG local controller connection to MG central controller. (b) CB status and voltage/frequency data transfer to central controller.

TABLE III
COMPARISONS OF EXISTING WIRELESS COMMUNICATION TECHNOLOGIES

Specifications	ZigBee	WiFi	WiMax	Bluetooth	Cellular
Low-cost device	✓			✓	
Less complexity	✓			✓	
Point-to-multi point connections	✓	✓	✓		✓
Direct connection to sensor/meter	✓			✓	
Low consumption	✓			✓	
Flexible for expansion	✓	✓		✓	
Encryption code	✓	✓	✓		

III. ZigBee Communication in MGs

ZigBee is an emerging wireless communication technology. It has several advantages over other existing wireless communication technologies which make it a better choice for MG applications. These advantages are as follows:

1) low-cost device compared to others [16];
2) less complexity for the users [20], [24];
3) flexibility for expansion in future [26];
4) possibility for multipoint interconnections [18], [19];
5) possibility of direct connection to any sensor, meter and actuator in MG [21], [23];
6) possibility of using encryption codes for enhancing the system security [9];
7) possibility of developing codes to prevent interference with other wireless communication signals [22];
8) low consumption device [11], [16] and therefore suitable for MGs that are usually in remote areas;
9) covering an area of 300–1500 m [28] which is further expandable by repeaters.

A comparison between different existing wireless communications technologies and the above-mentioned characteristics is presented in Table III. From this table, it can be seen that ZigBee is the most preferred technology for future MGs.

In terms of communication capabilities, there are two types of ZigBee devices, i.e., full function device (FFD) and reduced function device (RFD) [29]. An RFD has the capability to connect to sensors, actuators, and meters; however, it does not have the capability to communicate with other RFDs. On the other hand, an FFD has the capability to communicate with other FFDs as well as the sensors, actuators and meters [29]. The RFD acts as a ZigBee end-device, whereas the FFD can act as a router or a coordinator. The router is used for data routing or communication with other routers or coordinators, extending the covered area as well as strengthening the transmitted signals [11]. The coordinator is used to establish and manage the network.

The sensors/meters/actuators in one DG can be connected directly to the local controller through either of analog-to-digital converters, general purpose input–output, or serial communication [23]. The received data and any processed outputs can then be transmitted by the RFD, which is connected to the local controller. The transmitted data by the local controller of the DG will be received by the MG central controller through the FFD. This is shown in Fig. 3(a). Alternatively, the sensors/meters/actuators can be connected directly to an RFD which transmits the data to the MG central controller. This is applicable for measurements from the CB and power distribution feeders where no significant computation and control process is required. This is shown in Fig. 3(b).

The number of sensors, actuators, and meters in the MG can be massive and scattered, thus a network topology is required to handle the communication in a large area with numerous end user devices. ZigBee can operate in star, tree, and mesh network topologies as well as any combination of them [29]. In this paper, a star topology is considered for the network.

Every Zigbee network is characterized by a 64-bit unique address, referred to as personal area network (PAN), which is managed by the coordinator [29]. For ZigBee technology, it is allowed to build some communication network clusters in the same PAN network. This is a possible solution when one DG unit is composed of numerous smaller DGs, distributed over a vast area. An example can be wind turbines distributed within a wind farm or numerous photovoltaic cells distributed over a photovoltaic farm. The main advantage of a multicluster topology is expanding the coverage area, while its main disadvantage is the increase of data latency [13]. Fig. 4 schematically shows an example of a ZigBee-based multicluster communication network for the MG.

An important parameter to be considered in multicluster communication networks is the time occupation duty

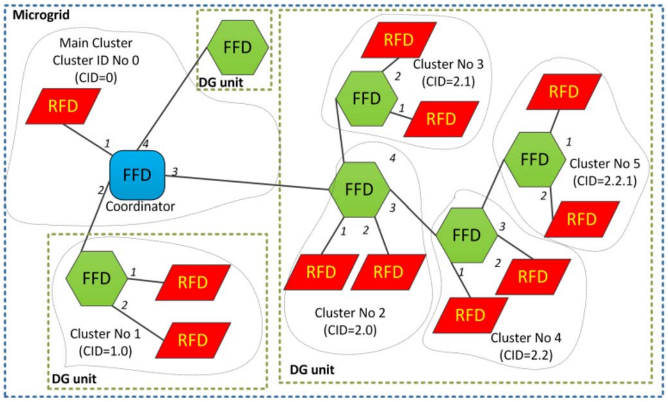

Fig. 4. ZigBee-based multicluster communication network for the MG.

ratio (TODR) that is the time period which each ZigBee device can take to transmit data to the coordinator. This duty ratio depends on the number of ZigBee-based clusters within the MG. Since the time allocated for each Zigbee device within the MG is equal, for the network of Fig. 4, TODR is calculated from

$$\mathrm{TODR}(\%) = \frac{100}{n_{\mathrm{dev}}^{CID} \times n_{\mathrm{dev}}^{CID-1} \times n_{\mathrm{dev}}^{CID-2} \times \cdots \times n_{\mathrm{dev}}^{0}} \tag{1}$$

where n_{dev}^{CID} is the number of ZigBee devices in the same cluster while the n_{dev}^{CID-1} represents the number of ZigBee devices in its upper cluster and n_{dev}^{0} is the number of ZigBee devices in the coordinator's cluster (main cluster).

As an example, based on (1), for each device in the main cluster (CID = 0) of Fig. 4, TODR of transferring data is

$$\mathrm{TODR} = \frac{100}{n_{\mathrm{dev}}^{0}} = \frac{100}{4} = 25\%$$

while, this ratio for each device in the clusters with CID = 1.0 and 2.2.1 are, respectively,

$$\mathrm{TODR} = \frac{100}{n_{\mathrm{dev}}^{CID=1.0} \times n_{\mathrm{dev}}^{0}} = \frac{100}{2 \times 4} = 12.5\%$$

$$\mathrm{TODR} = \frac{100}{n_{\mathrm{dev}}^{CID=2.2.1} \times n_{\mathrm{dev}}^{CID=2.2} \times n_{\mathrm{dev}}^{CID=2.0} \times n_{\mathrm{dev}}^{0}} = \frac{100}{2 \times 3 \times 4 \times 4} = 1.04\%.$$

From this example, it is seen that the TODR of an RFD in the cluster with CID = 1.0 for transferring data to the coordinator is 12 times higher than an RFD in the cluster with CID = 2.2.1. Therefore, the RFDs should be placed in different clusters based on the importance and frequency of data transmission to the coordinator. Based on this concept, the RFDs which transfer data with the following characteristics should be placed in the 1st/2nd cluster:

1) data transmitted frequently;
2) data transmitted to the coordinator immediately;
3) data affecting the whole control system of the MG;
4) data utilized for emergency purposes.

Hence, the voltage magnitude, angle and frequency, active/reactive power, and the states of the CBs should be within the 1st/2nd cluster. This paper focuses only on the data management scheme of these sets of data.

However, the data from the RFDs with the following characteristics can be placed in the farther clusters:

1) data sent for monitoring purpose only;
2) data with wide tolerance of data packet error;
3) data with low precision;
4) data affecting the local controllers only.

Hence, if the data such as weather forecasting info (e.g., the sun radiation, ambient temperature, wind speed, etc.) or the SoC of the batteries need to be transferred to the MG central controller, the relevant RFDs can be located in farther clusters.

IV. Data Management in MG

The number of data to be monitored and transferred in an MG depends on the number of the DGs within the MG. In addition, some DGs might have a particular set of data to be monitored and transmitted such as the weather data. Consequently, the number of data to be transferred in the MG can be very large. Since the data transfer rate of ZigBee is only up to 250 kbps, the data transmission in MGs should be carefully managed such that the network bandwidth can handle the data transactions.

The data management scheme proposed in this paper is based on defining a suitable time interval for transmitting the data and proper number of bits representing the data. Table IV shows the proposed number of bits for each data parameter in the MG. Some data need to be transmitted immediately such as the CB status. However, some data such as the voltage magnitude, angle, and frequency as well as the active/reactive power can be transferred in short intervals of ΔT. This interval needs to be defined based on the effect of the data on the performance of the MG and can be in the range of a few minutes.

In addition, to further reduce the number of data transmission, acceptable limits for the data variation can be defined such that the data are transmitted instantly only if the data exceed the defined limits of ΔL. Usually, the acceptable limits are only defined for the MG frequency (e.g., 49.5–50.5 Hz) and the voltage magnitude (e.g., 90%–110% of the nominal voltage). Based on ΔT and ΔL, the data management flowchart for each FFD is as shown in Fig. 5.

Based on IEEE Standard 802.15.4, data communication in ZigBee is formulated in the following four frames [29].

1) A beacon frame, used by a coordinator, to transmit beacons. This frame is consisted of $104 + (32 \text{ or } 80) + k + m + n$ bits where n is the number of beacon payload bits, m is the pending address field bits, and k is guarantee time slot field bits. Note that the (32–80) bits represent the address field.
2) A data frame, used for transferring all the data. This frame is consisted of $88 + (32 - 160) + N$ bits. The $(32 - 160)$ bits represent addressing field bits, N is the number of data payload bits where the maximum of data payload is 888 bits.

TABLE IV
DATA TO BE TRANSFERRED IN THE MG, THE NUMBER OF BITS AND THE BINARY/TEXT FORMATS FOR EACH DATA

Data	Data Value					Data Type	
	Range	Data steps	Step No	Bit No	Text digit	Binary	Text
Voltage Magnitude	0 - 500 V 0.00-20.00 kV	1 0.04	500 500	9 9	3 5	001	"VM"
Voltage angle (°)	0.0 - 360.0	0.1	3600	12	5	010	"VA"
Frequency (Hz)	0.0 - 60.0	0.1	600	10	4	011	"FR"
CBs	on, off	–	2	1	1	100	"CB"
Active Power	0 - 999 W 0 - 99 kW/MW	1 0.1	999 1000	10 10	3 4	101	"AP"
Reactive Power	0 - 999 W 0.0 - 99.0 kW/MW	1 0.1	999 1000	10 10	3 4	110	"RP"

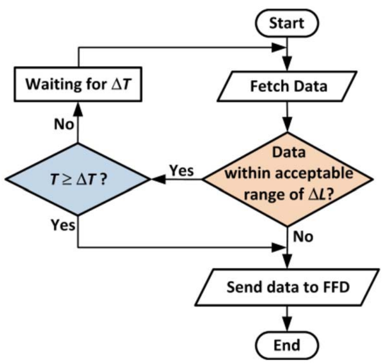

Fig. 5. Data management flowchart for RFDs.

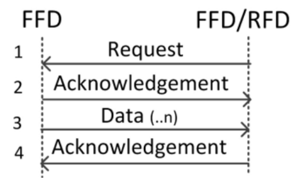

Fig. 6. Schematic of data request, transfer, and acknowledgement between the FFD/RFD and the coordinator.

3) An acknowledgment frame (ACK), used for confirming successful frame reception; this frame is consisted of 88 bits.
4) The medium access control (MAC) command frame which is used for handling all MAC peer entity control transfers. This frame is consisted of $96 + (32 - 160) + u$ bits where u is the command payload bit.

The communication between the FFD/RFDs and the coordinator (in nonbeacon network) starts by the coordinator requesting data from the FFD/RFDs. Then, the RFD/FFDs confirm by transmitting an ACK and the requested data. After receiving the data, the coordinator transmits the ACK to the FFD/RFDs. The schematic of this communication sequence is illustrated in Fig. 6.

Based on IEEE Standard 802.15.4, ZigBee devices are available with 868, 915 MHz, and 2.45 GHz carrier frequencies. The lower carrier frequency usually has longer area coverage, e.g., the 2.45 GHz ZigBee from the Xbee-Pro from Digi International Inc., can cover an area up to 1.5 km, while the 868 and 915 MHz ZigBees from the same manufacturer can cover an area up to 40 and 14.5 km, respectively [28]. The data modulation technique for the 868 and 915 MHz ZigBees is binary phase-shift keying (BPSK) while for the 2.45 GHz ZigBee is offset quadrature phase-shift keying (OQPSK). The data transfer rate for the 868, 915 MHz, and 2.45 GHz ZigBees is respectively 20, 40, and 250 kbps [29].

In 2.45 GHz ZigBee, every 4 bits of data needs to be mapped into one symbol and each symbol is then mapped into a 32-bit-chip-PN sequence. In 868 and 915 MHz ZigBees, each data bit needs to be mapped into a symbol and each symbol is then mapped into a 15-bit-chip-PN-sequence [29]. As an example, to transmit the voltage magnitude of 220 V, measured in the MG, from RFD to FFD using 2.45 GHz ZigBee, first the 220 decimal digits need to be coded into binary digit (i.e., 1101 1100). Then, the binary digit should be mapped into symbol and each symbol to be mapped into chip-PN sequence. Fig. 7 schematically shows the data modulation processes from binary digit into a symbol and then into chip-PN sequence before spreading in the form modulated signal.

The data to be transferred should be coded such that it represents data type (i.e., voltage magnitude, voltage angle, active power, reactive power, frequency, and CB status), data dimension (e.g., kilo and mega), data value (e.g., 220), RFD or FFD number, channel number (if there is more than one sensor/actuator/meter connected to a single RFD), and DG number in the MG. All these data need to be mapped into data payload section which has the maximum of 888 number of bits [29].

Data payload code can be represented in binary or text formats [30]. As an example, voltage magnitude of 220 V in decimal digits can be represented by binary code of 1101 1100 or as text characters of 220. The binary format can be processed faster by digital devices such as microcontroller and has less number of bit representations. However, the text format has more flexibility for expanding the network devices and data transactions in the MG. In addition, the binary format can be directly converted to the symbol and then into OQPSK or BPSK modulator, whereas the text format first needs to be converted into binary code using the well-known American Standard Code for Information Interchange code [30] and then into a symbol.

TABLE V
BINARY AND TEXT FORMAT CODING FOR DEFINING THE NUMBER OF DATA FOR THE GRID/DG UNITS, EACH RFD/FFD AND THEIR CHANNELS

Data	Data Code Binary	Data Code Text	Device	Data Code Binary	Data Code Text	Channel	Data Code Binary	Data Code Text
Grid	0000	"Grid"	RFD/FFD-1	001	"Dev1"	Ch-1	01	"Ch1"
DG-1	0001	"DG01"	RFD/FFD-2	010	"Dev2"	Ch-2	10	"Ch2"
DG-2	0010	"DG02"	RFD/FFD-3	011	"Dev3"	Ch-3	11	"Ch3"
DG-3	0011	"DG03"	RFD/FFD-4	100	"Dev4"	Ch-4	00	"Ch4"
….			….					
DG-15	1111	"DG15"	RFD/FFD-8	000	"Dev8"			

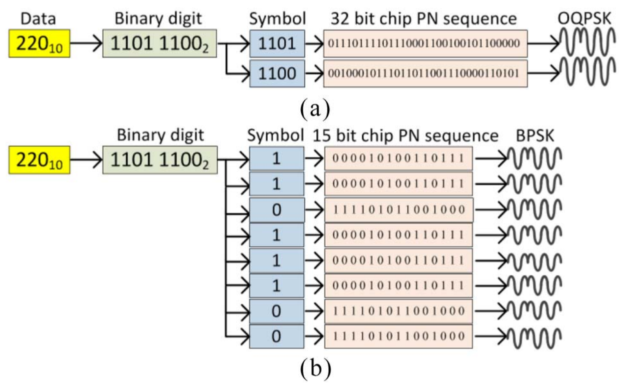

Fig. 7. Example illustrating the steps of modulating "220 V" in ZigBee with a carrier frequency of (a) 2.45 GHz and (b) 868 or 915 MHz.

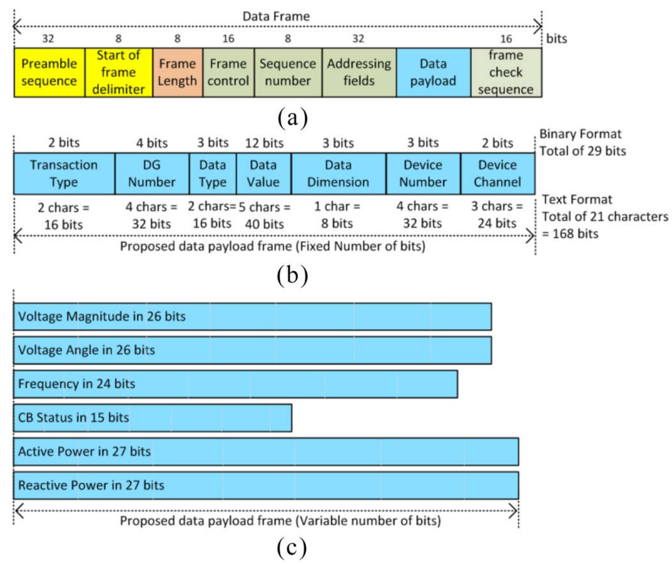

Fig. 8. (a) Standard data frame for ZigBee. (b) Proposed data payload structure for fixed number of bits for each parameter. (c) Proposed data payload structure for variable number of bits for each parameter.

Data transaction required in the MG can be classified as follows.

1) Data transfer where RFD sends data to FFD/coordinator.
2) Data request transaction, where the coordinator request data value or status from the RFD (e.g., the coordinator needs data of the generated active power from a DG).
3) Command transaction, where the coordinator sends a command to the RFD (e.g., the coordinator requests RFD to open/close a CB).

To define the transaction type among the above three options, a special code needs to be developed in binary or text formats. As an example, the developed code can represent data value, data request, and command transactions respectively by 01, 10, and 11 in binary format or by "VL," "RQ," and "CM" characters in text format. Similarly, each data type can be defined in binary or text format as shown in Table IV. Similarly, the commonly used dimensions of $10^0 - 10^6$ can be represented, respectively, as 000, 001, 010, 011, 100, 101, and 110 in binary format or "E," "1," "2," "K," "4," "5," and "M" in text format.

To measure the six required data from each MG (i.e., voltage magnitude, angle and frequency, active/reactive power, and CB status), maximum of six RFDs may be required. In addition, it is expected that no more than four sensors/meters/actuators are connected to the same RFD. Hence, a maximum of 3 bits are required for the RFD number and 2 bits for the channel number. The number of DGs within an MG defines the number of bits that are required to define it. As an example, assuming the number of DGs is less than 15, four bits are required to define the number of DGs in the MG. This coding in binary and text formats is given in Table IV. This data payload coding is then utilized within the data payload section of the standard ZigBee data frame.

There are two options to transmit the data. The first method is based on considering a fixed number of bits or characters for each parameter. This method is easier to be recognized by system and RFD/FFDs; however, it results in longer data bit lengths. The second method is based on having a different number of bits for each parameter, depending on the number of bits or characters defined for each parameter, as introduced in Tables IV and V. The main advantage of the second method is the less number of bits and hence a shorter processing delay. Fig. 8(a) shows the standard data frame for ZigBee where these two methods are shown schematically in Fig. 8(b) and (c). In this research, both of these methods are utilized and their processing delay times are compared. The period of data frame in ZigBee is the sum of the period of data payload and the period of other transmitted parameters such as preamble sequence, start of frame delimiter, etc., as shown in Fig. 8(a).

As an example, let us assume a voltage sensor that is connected to channel-2 of RFD-5 in DG-4 measures a voltage magnitude of 220 V. The data to be transmitted is coded as shown in Fig. 9. From this figure, it can be seen that the 220 V measurements can be transmitted by 26 bits when

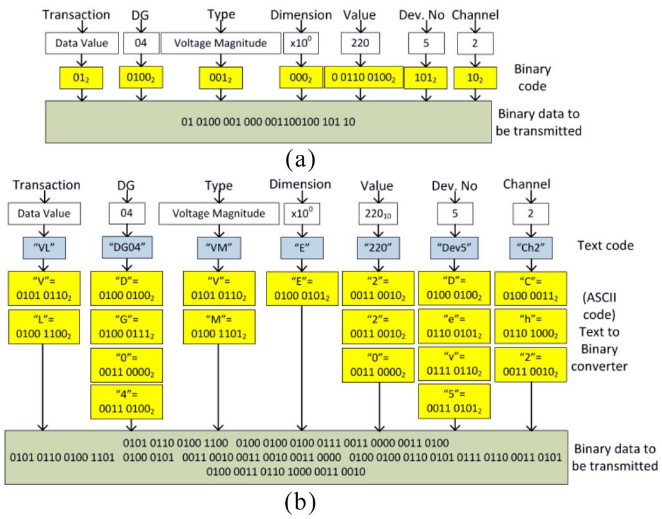

Fig. 9. Example illustrating how the output of a voltage sensor is coded within the data payload section of the ZigBee data frame based on the proposed (a) binary format and (b) text format.

binary format is utilized or by 152 bits when text format is used.

By applying the above discussed data management, the number of data transmission in the MG is significantly reduced without causing any difficulty in MG normal operation.

V. Data Transmission Delay

The time to transfer each bit by ZigBee devices depends on the data transfer rate. This time can be calculated as $T_{\text{Bit}} = 1/\text{data rate}$. Hence, T_{Bit} is equal to 4, 25, and 50 μs for the 2.45 GHz, 915, and 868 MHz ZigBee devices, respectively.

The required time to transfer a symbol (T_{Symbol}) can be calculated as $T_{\text{Symbol}} = T_{\text{Bit}} \times$ number of bits in each symbol. Hence, T_{Symbol} of 2.45 GHz ZigBee is $T_{\text{Bit}} \times 4$ bits $= 16$ μs; however, T_{Symbol} when using 915 and 868 MHz ZigBees are, respectively, $T_{\text{Bit}} \times 1$ bit $= 25$ μs and $T_{\text{Bit}} \times 1$ bit $= 50$ μs.

The total processing time for the data payload ($T_{\text{DataPayload}}$) is calculated as

$$T_{\text{DataPay load}} = T_{\text{Symbol}} \times \text{ceiling}\left(\frac{\text{number of binary digits}}{\text{number of bits in each symbol}}\right) \quad (2)$$

where the number of bits for a symbol is 4 for the 2.45 GHz ZigBee and one for the 915 and 868 MHz ZigBees.

As an example, the processing time of transmitting the data payload of 220 V, shown in Fig. 9, for ZigBees with different carrier frequencies and different formats are listed in Table VI.

Assuming minimum number of bits is used for the address fields (i.e., 32 bits based on [29]), the total processing time for transferring the data frame ($T_{\text{DataFrame}}$) is calculated as

$$T_{\text{DataFrame}} = T_{\text{DataPayload}} + T_{\text{DF}} \quad (3)$$

TABLE VI
NUMERICAL COMPARISON OF DATA PROCESSING TIME [MS] WHEN USING ZIGBEES WITH DIFFERENT CARRIER FREQUENCIES AND DIFFERENT FORMATS

	Binary Format	Text Format
	2.45 GHz	
$T_{DataPayload}$	16µs × ceiling(26/4) = 0.112	16µs × ceiling(152/4)=0.608
	915 MHz	
$T_{DataPayload}$	25µs × 26 bits = 0.65	25µs × 152 bits = 3.8
	868 MHz	
$T_{DataPayload}$	50µs × 26 bits = 1.3	50µs × 152 bits = 7.6

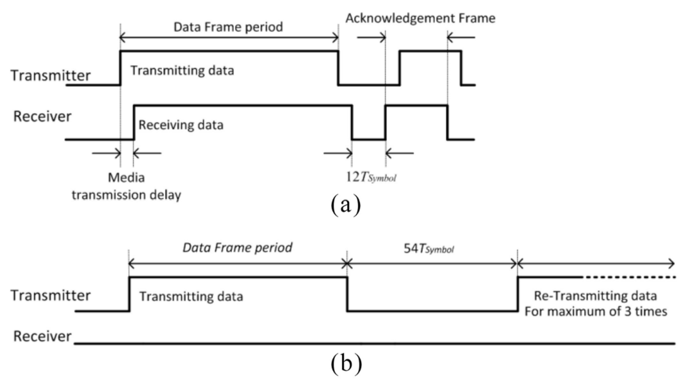

Fig. 10. Schematic of data transmission in ZigBee. (a) Successful and (b) unsuccessful data transaction.

where T_{DF} is the processing time for the other sections of the data frame (i.e., preamble sequence, start of frame delimiter, frame length, frame control, sequence number, addressing field, and frame check sequence sections). T_{DF} is 480, 3000, and 6000 μs, respectively, for 2.45 GHz, 915, and 868 MHz ZigBee.

After a successful data transaction, the receiving FFD sends an ACK. The processing time of an ACK is 352, 2200, and 4400 μs, respectively, for 2.45 GHz, 915, and 868 MHz ZigBees. The complete data transmission in ZigBee is started by transmitting the data frame by the transmitter followed by an ACK received from the receiver. The receiver sends back the ACK after a period of 12 T_{Symbol}. The waiting time since the data is fully transmitted until receiving the ACK has a maximum of 54 T_{Symbol} [29]. The successful data in ZigBee is illustrated as shown in Fig. 10(a).

If the transmitter does not receive any an ACK within this period, it resends the data frame to the receiver again. The transmitter will retry to transmit this data maximum of three times [29]. If the transmitter still does not receive an ACK, it generates a MAC sublayer management entity-COMM-STATUS indication with a status of NO_ACK [29]. The unsuccessful data transmission in ZigBee is illustrated as shown in Fig. 10(b).

VI. Numerical Analysis Results

The time delay for transmitting the numerical values of the measurements from sensors to the MG central controller or data commands from the central controller to the local controllers of each DG is of high importance. In this section, the time delay is calculated and presented as the processing time required to transfer a data frame ($T_{\text{DataFrame}}$). An example is

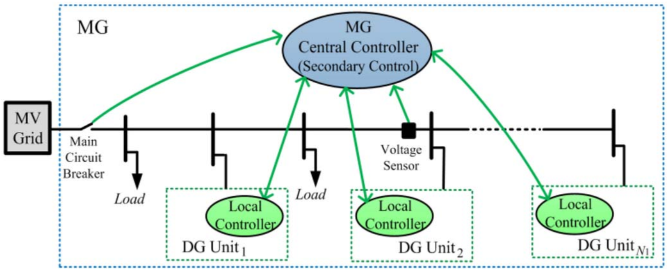

Fig. 11. Schematic of the MG network under consideration.

presented below to numerically analyze the communication delay and the number of transmitted symbols as a function of number of DG units in an MG, ZigBee carrier frequencies, and different proposed data payload formats.

Let us consider the MG structure of Fig. 11 with N_1 converter-interfaced DGs and a few distributed loads. The DGs are connected through voltage source converters (VSC) and associated filters. The detailed discussion on the DG type, VSC and filter structure and its control system are presented in [25] and not repeated here. The local controller of each DG unit transmits the average output active and reactive power of the DG to the MG central controller. In addition, the local controller of each DG unit receives the voltage and angle set-points from the MG central controller. The MG central controller also receives the status of the MG main CB from the CB as well as the voltage magnitude, angle and frequency from a voltage sensor installed at the MG feeder.

Fig. 12(a) shows the comparison of $T_{\text{DataFrame}}$ between 2.45 GHz, 915, and 868 MHz ZigBees for transferring one set of data (i.e., voltage magnitude, voltage angle, frequency, active and reactive power, and CB status) for different number of DGs in the MG. These results are for fixed number of bits for all data in the payload section. The results indicate that $T_{\text{DataFrame}}$ is around 48 and 86 ms, respectively, when using binary and text formats for 2.45 GHz ZigBee. However, when using 915 and 868 MHz ZigBees, $T_{\text{DataFrame}}$ becomes five and ten times more than that of the 2.45 GHz ZigBee. From this figure, it can be seen that transmitting 15 sets of the above-mentioned data approximately takes 48.03 ms when using binary coding with 2.45 GHz Zigbee.

Fig. 12(b) shows the comparison between $T_{\text{DataFrame}}$ of variable and fixed number of bits of data in the payload section of the data frame. The results are shown for both binary and text formats when using 2.45 GHz ZigBee. The results indicate that in text format, $T_{\text{DataFrame}}$ is 1.8 times larger than the binary format. However, $T_{\text{DataFrame}}$ is approximately 7% larger when using fixed number of bits compared to variable number of bits.

The maximum number of symbols that can be transmitted in ZigBee network is 62.5, 40, and 20 k symbols per second when using, respectively, the 2.45 GHz, 915, and 868 MHz ZigBees. Fig. 12(c) shows that the total symbols transmitted in MG is 1112 in binary format and almost three times more when using text format, for a 2.45 GHz ZigBee. This result indicates that when transmitting 15 sets of the above-mentioned data, ZigBee still has the capability to transfer approximately 56 times and 18 times more data, respectively, in binary and text formats.

Fig. 12(d) shows the number of symbols required for transmitting the above-mentioned data when using 2.45 GHz, 915, and 868 MHz ZigBees. From this figure, it can be seen that the number of symbols required for transmitting 15 sets of the above-mentioned data when using a 868 MHz ZigBee and text format is very close to the maximum limit of ZigBee technology. However, the number of symbols when using 2.45 GHz and 915 MHz ZigBees in the same format is still, respectively, 5.5% and 34.8% of the maximum limit.

Table VII shows the processing time (i.e., $T_{\text{DataPayload}}$ and $T_{\text{DataFrame}}$) of each data with variable and fixed number of bits in the data payload section, when using 2.45 GHz ZigBee. From this table, it can be seen that when using the fixed number of bits for all data, $T_{\text{DataFrame}}$ is 0.608 (in binary format) or 1.088 ms (in text format). However, when using the variable number of bits for the data, the minimum $T_{\text{DataFrame}}$ is 0.544 (in binary format) or 0.992 ms (in text format) while its maximum is 0.592 (in binary format) or 1.152 ms (in text format).

VII. Communication Delay Effect on MG Performance

To evaluate the dynamic performance of an MG consisting of converter-interfaced DGs where communication delay is considered in the MG hierarchical control system, a simulation study is carried out in PSCAD/EMTDC.

Let us consider the MG network of Fig. 11 with only two DGs (i.e., DG1 and DG2). Let us assume that it is desired to maintain the output power ratio of DG1 versus DG2 as 1:2. The MG is considered initially at steady-state and autonomous condition, with a total load demand of 0.41 p.u. where 1 p.u. is 6 kVA. At $t = 0.5$ s, the MG load is increased to 1 p.u. and at $t = 1$ s decreased to 0.53 p.u. At $t = 1.5$ s, the load is further decreased to 0.17 p.u. Following every load change, the DGs update their output powers accordingly and the voltage magnitude and frequency in the MG feeder is modified. The MG dynamic operation and control is summarized in the Appendix. The MG parameters are listed in Table B1 in the Appendix.

A. *Case-1: MG Performance Without Any Delay*

First, let us assume there is no communication delay ($T_{\text{DataFrame}} = 0$). The total active power demand of the loads of the MG is shown in Fig. 13(a). The output active power ratio among the two DGs is maintained as 1:2, as shown in Fig. 13(b). The RMS of the voltage of MG feeder (V_{MG}) is within the acceptable limits for all load changes, as shown in Fig. 13(c).

B. *Case-2: Droop Control Within the MG Central Controller*

As discussed in Section II, the droop control should be located within the local controller of each DG. If the droop control is considered as a module of the MG central controller

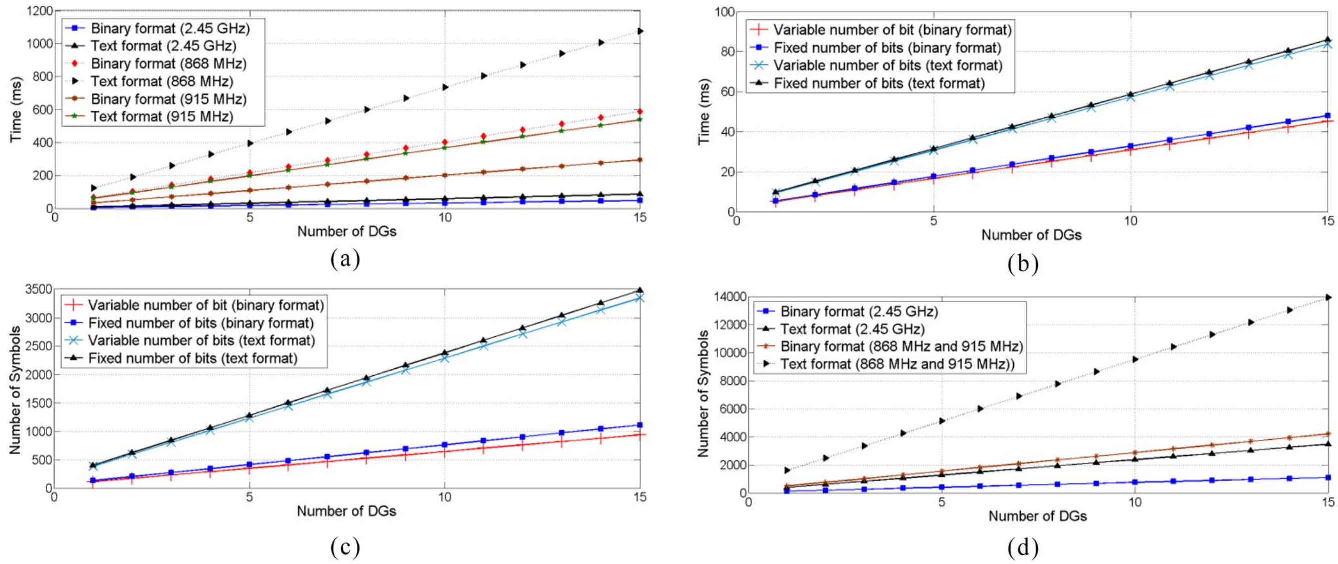

Fig. 12. Numerical analysis results. (a) $T_{\text{DataFrame}}$ in 2.45 GHz and 868 MHz ZigBees (fixed number of bit based). (b) $T_{\text{DataFrame}}$ of 2.45 GHz ZigBee. Number of transmitted symbols in (c) 2.45 GHz ZigBee and (d) 2.45 GHz, 915, and 868 MHz ZigBees (fixed number of bit based).

TABLE VII
NUMBER OF BITS AND CHARACTERS FOR EACH PARAMETER IN BINARY AND TEXT FORMATS AND THE REQUIRED DATA PAYLOAD AND DATA FRAME PROCESSING TIMES

Data		Total Number of		$T_{DataPayload}$ (ms)		$T_{DataFrame}$ (ms)	
		Bits	Characters	Bits	Characters	Bits	Characters
Variable number of bits	Voltage Magnitude	26	21	0.112	0.672	0.592	1.152
	Voltage Angle	26	20	0.112	0.64	0.592	1.12
	Frequency	24	19	0.096	0.608	0.576	1.088
	Active Power	27	20	0.112	0.64	0.592	1.12
	Reactive Power	27	20	0.112	0.64	0.592	1.12
	CB Status	15	16	0.064	0.512	0.544	0.992
Fixed number of bits		29	21	0.128	0.672	0.608	1.152

(i.e., centrally managed droop control), the data communication system is required to transfer the output active and reactive power of each DG to the central controller and return the voltage magnitude and angle instantaneously to the DG local controllers. The ZigBee devices in the central controller and the DG local controllers may transmit and receive only one data at a time. Therefore, for the MG system of Fig. 11 which contains two DGs and each DG needs to transmit two data (i.e., active and reactive power) and receive two data (i.e., voltage magnitude and angle), the total processing time for transmitting and receiving data in ZigBee (shown in Fig. 10) with the fastest ZigBee technology (i.e., 2.45 GHz), and assuming a fixed binary format is two DGs $\times$ four data $\times (0.608 + 0.544)$ ms $= 9.216$ ms where 0.608 ms is $T_{\text{DataFrame}}$ for a single data (from Table VII) and 0.544 ms is the sum of the period of waiting time (i.e., 12 $T_{\text{Symbol}} = 12 \times 16\ \mu\text{s} = 192\ \mu\text{s}$) plus the ACK processing time (i.e., 352 μs from Section V). Thus, 9.216 ms is the minimum communication delay for an MG with only two DGs. It is to be noted that in this calculation, the controller processing time and the media transmission delays (in Fig. 10) are still ignored. This delay will be higher if the number of DGs is increased or if 868 or 915 MHz ZigBees or text format are utilized.

Now, a fixed delay of 0.5 ms is applied in the MG system of case-1 to transfer the active and reactive power from the local controller of each DG to the MG central controller and another 0.5 ms to transfer the voltage magnitude and angle from the MG central controller to the local controller of each DG. The simulations results are shown in Fig. 14. It can be seen that the considered delay time does not lead to dynamic maloperation of the DGs. By increasing the delay time to more than 1 ms, the dynamic operation of the DGs are affected. As an example, the results of the system with 4 and 10 ms delay are shown, respectively, in Figs. 15 and 16. It can be seen that for a delay of 4 ms, a deviation in the voltage magnitude and output powers of the DGs are observed while for a delay of 10 ms, the MG system becomes unstable.

C. Case-3: Droop Control Within the DG Local Controller

In case-2, it has been demonstrated that a centrally managed droop control will fail due to high communication delay. Now, let us assume that the droop control is located within the local controller of each DG, as discussed in Section II and the MG central controller is only responsible for regulating the network voltage and frequency within the standard limits, only if they are violated. It is to be noted that this is a discrete process

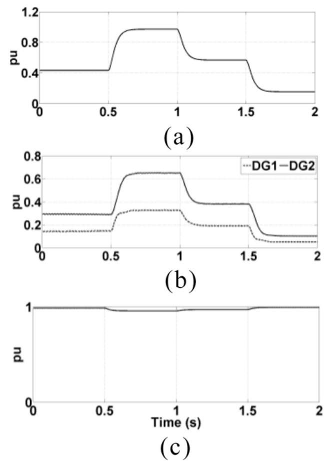

Fig. 13. MG performance without any communication delay (case-1). (a) Load active power. (b) DGs active power. (c) V_{MG} RMS.

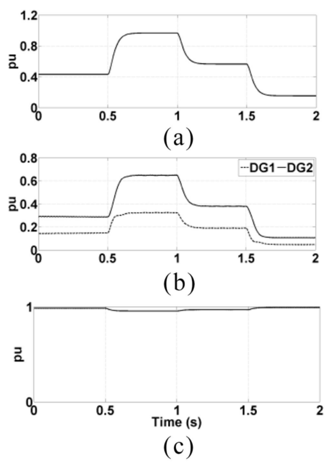

Fig. 14. MG performance assuming 0.5 ms communication delay (case-2). (a) Load active power. (b) DGs active power. (c) V_{MG} RMS.

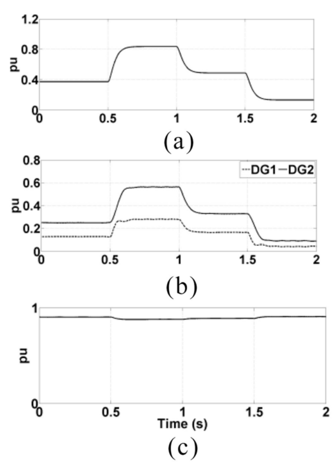

Fig. 15. MG performance assuming 4 ms communication delay (case-2). (a) Load active power. (b) DGs active power. (c) V_{MG} RMS.

with a sampling time of a few minutes. The voltage magnitude and frequency are monitored in the MG feeder using a voltage sensor. The total communication delay for transferring these two data from the voltage sensor to the MG central controller

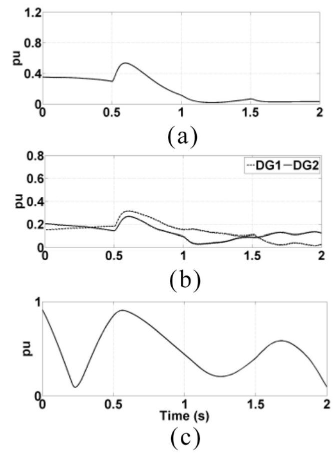

Fig. 16. MG performance assuming 10 ms communication delay (case-2). (a) Load active power. (b) DGs active power. (c) V_{MG} RMS.

with the slowest ZigBee technology (i.e., 868 MHz) and fixed text format is two data $\times\,(14.4 + 5)$ ms $= 38.8$ ms where 14.4 ms is $T_{\text{DataFrame}}$ for a single data and 5 ms is the sum of waiting time and an ACK (i.e., 4400 μs from Section V). Considering the same processing time when the MG central controller transfers back the new references for voltage magnitude and angle, the total communication delay will be at least 2×38.8 ms $= 77.6$ ms. However, as this process has a discrete operation with a large time step of few minutes, this delay will not affect the system operation.

D. Case-4: Communication Delay for Transferring MG Main CB Status

As discussed in Section II, the status of the MG main CB should be immediately transferred to the local controller of each DG so that the DGs can update their operation mode if the MG changes its mode of operation from grid-connected to autonomous and vice versa. The CB status is required to be transferred to the MG central controller and the MG central controller passes this information to the local controller of each DG immediately. In such a case, the total communication delay for the MG system of Fig. 11 with two DGs with the slowest ZigBee technology (i.e., 868 MHz) and fixed text format for one data is $(14.4 + 5)$ ms $= 19.4$ ms. The communication delay includes transmission processing time from CB controller to MG central controller, and transmission processing time from MG central controller to local controller of each DG. Thus, this data communication delay is at least two data transfer $\times$ 19.4 ms $= 38.8$ ms. It is to be noted that this delay will not rise if the DGs number increases in the MG.

Now, let us consider the network of case-1. It is assumed that the MG is initially at steady-state condition and grid-connected. At $t = 0.4$ s, the MG main CB opens and it falls into autonomous mode of operation. The system of case-1 is simulated assuming a zero and 40 ms communication delay for transferring the MG main CB status to the local controller of the DGs. The network voltage is shown in Fig. 17. As it can be seen from this figure, the DGs dynamic operation does not fail even for a 40 ms delay.

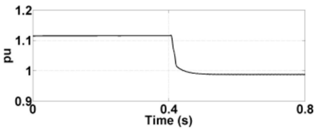

(a)

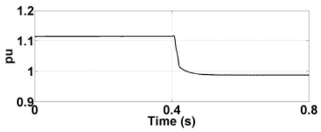

(b)

Fig. 17. MG performance assuming a zero and 40 ms communication delay for transferring MG main CB status to the local controller of DGs (case-4). (a) V_{MG} RMS (no delay). (b) V_{MG} RMS (40 ms delay).

VIII. Conclusion

A ZigBee-based wireless data communication system is presented in this paper for future MGs. The proposed communication system is responsible for transmitting several electrical parameters (i.e., voltage magnitude, angle and frequency, active/reactive power, and the CB status) from the local controller of every DG to the MG central controller as well as the reference for voltage magnitude and angle and CB status from the central controller to the local controller of each DG unit. ZigBee standard data frame is utilized for transmitting the data while a new coding is presented for the data payload section of this frame. The new coding can represent each of the above-mentioned data, their values, dimensions and the origin of the data (sensor, meter, etc.) in binary or text formats. The data payload section may be composed of a fixed number of bits or a variable number of bits, as proposed in this paper. The selection of the binary/text format, fixed/variable number of bits for the data payload, and the carrier frequency effects the data transmission delay. Through several numerical analyses, a comparison is provided on the expected data transmission delay as well as the maximum number of symbols used for the data transaction in MGs with several DG units. These analyses are carried out for the above-mentioned data sets and the relevant transmission delays are calculated in each format/coding configuration. From these analyses, it can be seen that to cover a vast area, ZigBees with carrier frequency of 868 or 915 MHz are required; however, the data transmission delay is increased while for shorter distances, a 2.45 GHz ZigBee can be used which has a much smaller data transmission delay. Through the PSCAD/EMTDC-based simulations, it was shown that the droop control system needs to be located within the local controller of each DG unit; otherwise, there is a great possibility of system instability due to the communication delays, even for the ZigBees with fastest processing time. It was also shown that the communication delay for transferring the set-points of the droop control from the central controller and the MG main CB status to the local controller of each DG does not affect the dynamic performance of the MG system even for the ZigBees with slowest processing time.

Appendix

A. MG Dynamic Operation and Control

The considered DG units in this paper are connected to the MG by VSC. The VSCs operate in voltage control strategy. The VSC and its associated filter structure as well as its control strategy are presented in [25] and not repeated here.

When MG is in grid-connected mode, the DGs operate at the maximum power point (or rated) conditions. However, as the MG falls into autonomous mode, the status of the MG main CB is transferred to the local controller of each DG unit through the MG central controller to change the local controller mode of operation. In autonomous mode, the output power of the DG units are controlled by $P - \delta$ and $Q - V$ droop control equations as [25]

$$\begin{aligned} |V| &= V_{\text{rated}} + n\,(Q_{\text{rated}} - Q) \\ \delta &= \delta_{\text{rated}} + m\,(P_{\text{rated}} - P) \end{aligned} \tag{A1}$$

where $|V|$ and δ are, respectively, the magnitude and angle of the voltage at the output of VSC of the DG unit, P and Q are, respectively, the average active and reactive power at the DG connection point to the network, m is the coefficient of the $P - \delta$ droop equation, and n is the coefficient of the $Q - V$ droop equation. In (A1), it is assumed that $P_{\text{rated}} = P_{\max}/2$ and $Q_{\text{rated}} = 0$.

In [25], it is shown that for a proper power sharing ratio control among parallel DG units in an autonomous MG, it is required to satisfy the following equations:

$$\frac{P_2}{P_1} = \frac{P_{\text{rated},2}}{P_{\text{rated},1}} = \frac{m_1}{m_2}, \qquad \frac{Q_2}{Q_1} = \frac{Q_{\text{rated},2}}{Q_{\text{rated},1}} = \frac{n_1}{n_2}. \tag{A2}$$

As the network load is varied, the DGs automatically adopt their output power to supply the new load demand of the system. Hence, the voltage and frequency of the network is indirectly regulated by (A1).

If the network voltage and frequency fall beyond the acceptable predefined limits, the MG central controller will take action and adjust the set points of the droop controller for each DG. This process required a data transfer between the voltage sensor in the feeder to the MG central controller and from the central controller to the local controllers of each DG unit. The new set-points can be calculated as presented in [31].

B. Technical Parameters of the Network Under Consideration

The technical data of the MG under consideration in Fig. 11 are listed in Table B1.

TABLE B1
Technical Data of the Network Parameters of Fig. 11

MG network	400 Vrms L-L, 50 Hz			
MG feeder impedance	$R = 0.2\ \Omega$, L =10 mH			
	$P_{\max}$ [kW]	L_T [mH]	m [rad/kW]	n [V/kVAr]
DG1	2	2.72	3.1416	18
DG2	4	1.36	1.5708	9

References

[1] R. H. Lasseter and P. Paigi, "Microgrid: A conceptual solution," in *Proc. IEEE 35th Annu. Power Electron. Spec. Conf.*, Aachen, Germany, 2004, pp. 4285–4290.

[2] A. Sendin, "Communication technologies, networks and strategies for practical smart grid deployments: From substations to meters," in *Communication and Networking in Smart Grids*, Y. Xiao, Ed. Boca Raton, FL, USA: CRC Press, 2012, pp. 241–275.

[3] S. Yoon, S. Jang, S. Bahk, and Y. Kim, “Opportunistic routing for smart grid with power line communication access networks,” *IEEE Trans. Smart Grid*, vol. 5, no. 1, pp. 303–311, Jan. 2014.
[4] C. Zhang, W. Ma, and C. Sun, “A switchable high-speed fiber-optic ring net topology and its method of high-performance synchronization for large-capacity power electronics system,” *Int. J. Elect. Power Energy Syst.*, vol. 57, pp. 335–349, May 2014.
[5] N. Radhika and V. Vanitha, “Smart grid test bed based on GSM,” *Procedia Eng.*, vol. 30, no. 2011, pp. 258–265, 2012.
[6] A. Usman and S. H. Shami, “Evolution of communication technologies for smart grid applications,” *Renew. Sustain. Energy Rev.*, vol. 19, pp. 191–199, Mar. 2013.
[7] F. Gómez-Cuba, R. Asorey-Cacheda, and F. J. González-Castaño, “Smart grid last-mile communications model and its application to the study of leased broadband,” *IEEE Trans. Smart Grid*, vol. 4, no. 1, pp. 5–12, Mar. 2013.
[8] Y. Zhang *et al.*, “Distributed intrusion detection system in a multi-layer network architecture of smart grids,” *IEEE Trans. Smart Grid*, vol. 2, no. 4, pp. 796–808, Dec. 2011.
[9] T. Liu *et al.*, “A dynamic secret-based encryption scheme for smart grid wireless communication,” *IEEE Trans. Smart Grid*, vol. 5, no. 3, pp. 1175–1182, May 2014.
[10] N. Langhammer and R. Kays, “Performance evaluation of wireless home automation networks in indoor scenarios,” *IEEE Trans. Smart Grid*, vol. 3, no. 4, pp. 2252–2261, Dec. 2012.
[11] N. C. Batista, R. Melício, J. C. O. Matias, and J. P. S. Catalão, “Photovoltaic and wind energy systems monitoring and building/home energy management using ZigBee devices within a smart grid,” *Energy*, vol. 49, pp. 306–315, Jan. 2013.
[12] S. Ahmad, “Smart metering and home automation solutions for the next decade,” in *Proc. Int. Conf. Emerg. Trends Netw. Comput. Commun. (ETNCC),* Udaipur, India, 2011, pp. 200–204.
[13] C. Deng *et al.*, “Terrestrial-satellite hybrid backbone communication network for smart power grid,” *Energy Procedia*, vol. 12, pp. 27–36, Sep. 2011.
[14] Y. K. Chen, Y. C. Wu, C. C. Song, and Y. S. Chen, “Design and implementation of energy management system with fuzzy control for DC microgrid systems,” *IEEE Trans. Power Electron.*, vol. 28, no. 4, pp. 1563–1570, Apr. 2013.
[15] N. C. F. Tse, J. Y. C. Chan, W. H. Lau, J. T. Y. Poon, and L. L. Lai, “Real-time power-quality monitoring with hybrid sinusoidal and lifting wavelet compression algorithm,” *IEEE Trans. Power Del.*, vol. 27, no. 4, pp. 1718–1726, Oct. 2012.
[16] F. M. Sallabi, A. M. Gaouda, A. H. El-Hag, and M. M. A. Salama, “Evaluation of ZigBee wireless sensor networks under high power disturbances,” *IEEE Trans. Power Del.*, vol. 29, no. 1, pp. 13–20, Feb. 2014.
[17] J. Huang, H. Wang, Y. Qian, and C. Wang, “Priority-based traffic scheduling and utility optimization for cognitive radio communication infrastructure-based smart grid,” *IEEE Trans. Smart Grid*, vol. 4, no. 1, pp. 78–86, Mar. 2013.
[18] Y. Huang, A. Pang, and P. Hsiu, “Distributed throughput optimization for ZigBee cluster-tree networks,” *IEEE Trans. Parallel Distrib. Syst.*, vol. 23, no. 3, pp. 513–520, Mar. 2012.
[19] H. Y. Tung *et al.*, “The generic design of a high-traffic advanced metering infrastructure using ZigBee,” *IEEE Trans. Ind. Informat.*, vol. 10, no. 1, pp. 836–844, Feb. 2014.
[20] C. Tseng, “Coordinator traffic diffusion for data-intensive Zigbee transmission in real-time electrocardiography monitoring,” *IEEE Rev. Biomed. Eng.*, vol. 60, no. 12, pp. 3340–3346, Dec. 2013.
[21] Y. Zhang and Q. Li, “Exploiting ZigBee in reducing WiFi power consumption for mobile devices,” *IEEE Trans. Mobile Comput.*, vol. 13, no. 12, pp. 2806–2819, Dec. 2014.
[22] P. Yi, C. Zhou, and A. Iwayemi, “Developing ZigBee deployment guideline under WiFi interference for smart grid applications,” *IEEE Trans. Smart Grid*, vol. 2, no. 1, pp. 110–120, Mar. 2011.
[23] I. Hwang, D. Lee, and J. Baek, “Home network configuring scheme for all electric appliances using ZigBee-based integrated remote controller,” *IEEE Trans. Consum. Electron.*, vol. 55, no. 3, pp. 1300–1307, Aug. 2009.
[24] P. Valdastri, A. Menciassi, and P. Dario, “Transmission power requirements for novel ZigBee implants in the gastrointestinal tract,” *IEEE Rev. Biomed. Eng.*, vol. 55, no. 6, pp. 1705–1710, Jun. 2008.
[25] F. Shahnia, R. P. S. Chandrasena, S. Rajakaruna, and A. Ghosh, “Primary control level of parallel distributed energy resources converters in system of multiple interconnected autonomous microgrids within self-healing networks,” *IET Gener. Transmiss. Distrib.*, vol. 8, no. 2, pp. 203–222, Feb. 2014.
[26] I. Serban and C. Marinescu, “Control strategy of three-phase battery energy storage systems for frequency support in microgrids and with uninterrupted supply of local loads,” *IEEE Trans. Power Electron.*, vol. 29, no. 9, pp. 5010–5020, Sep. 2014.
[27] X. Lu, K. Sun, J. M. Guerrero, and J. C. Vasquez, “An improved droop control method for DC microgrids based on low bandwidth communication with DC bus voltage restoration and enhanced current sharing accuracy,” *IEEE Trans. Power Electron.*, vol. 29, no. 4, pp. 1800–1812, Apr. 2014.
[28] *XBee/XBee-PRO RF Modules*, Digi Int., Minnetonka, MN, USA, 2009.
[29] *IEEE Computer Society*, 1st ed. IEEE Standard 802.15.4, 2003.
[30] W. Stallings, *Data and Computer Communication*. Upper Saddle River, NJ, USA: Pearson Prentice Hall, 2007.
[31] R. P. S. Chandrasena, F. Shahnia, A. Ghosh, and S. Rajakaruna, “Secondary control in microgrids for dynamic power sharing and voltage/frequency adjustment,” in *Proc. Australasian Univ. Power Eng. Conf. (AUPEC)*, Perth, WA, Australia, 2014, pp. 1–8.

Authors’ photographs and biographies not available at the time of publication.